26th ABCM International Congress of Mechanical Engineering
November 22-26, 2021. Florianópolis, SC, Brazil

COB-2021-0109
DEVELOPMENT OF ROCKET MOTOR TRANSIENT THERMAL ANALYSIS SOFTWARE

Andres Gilberto Machado da Silva Benoit
João Vítor Bernardi Rohr
Department of Mechanical Engineering, Federal University of Santa Maria, Brazil.
andres.benoit@acad.ufsm.br, joao.rohr@acad.ufsm.br

João Felipe de Araujo Martos
Department of Mechanical Engineering, Federal University of Santa Maria, Brazil.
joao.martos@ufsm.br

Abstract. *Thermal analysis has a wide impact on overall success of aerospace applications, especially those that involve rocket motors. Nowadays, university rocket teams do not have means to early examine the motor thermal conditions and its behavior. In order to fulfill that, it was created a computational software with a graphical user interface (GUI) in which is presented the inputs and outputs for two analysis scenarios, first one considers one dimension discretization and occurs on the combustion chamber wall, the second has a two-dimensional approach and it is applied directly on the motor bulkhead. In addition, to calculate the heats and convection occurring in the chamber it was used the Newton's Law of Cooling and the transient Fourier Law. Notwithstanding, the solution method used was finite difference solved by explicit and implicit methods. Therefore, the explicit method exhibited a stable solution with similar behavior to that of the implicit solution, as expected from theory research. Also, a comparison with THERMCAS, other thermal analysis software was conducted and results revealed that the software built in this work has better accordance with real results.*

Keywords: *rocket, motor, thermal, analysis, student-built.*

1. INTRODUCTION

Rocket propulsion is a class of jet propulsion that produces thrust by ejecting matter, called the working fluid or propellant, stored entirely in the flying vehicle (Sutton and Biblarz, 2017). Rocket propulsion is the main way to access space for various purposes, such as putting telecommunication satellite in orbit or even human being to space station, and in the future for multi planetary flight (Turner, 2009). In order to overcome this challenges it is necessary to master the technology of rocket propulsion, and as a direct result of being capable of space exploration are not only economical development but also social and personal transformation (White, 2018).

Rocket propulsion may be organized in many categories (Humble *et al.*, 1995), and one of those is the solid rocket motor. According to (Sutton and Biblarz, 2017), a solid rocket motor (SRM) is composed of five basic elements, which are displayed in Fig. (1).

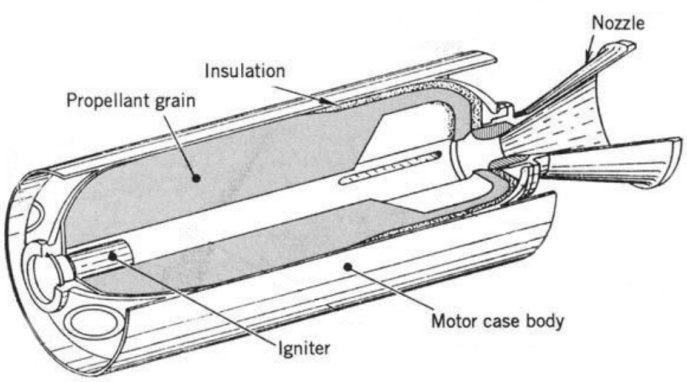

Figure 1. Solid Rocket Motor configuration. Adapted from: (Sutton and Biblarz, 2017).

Made either from metal or from composite materials (glass, kevlar and carbon fibers), the motor structure must be capable of withstanding the internal pressure resulting from the motor operation (Davenas, 1993). So maintaining the motor structural resistance is of prime importance once the motor operates with high temperature gases. The motor structure may be divided into two sections, the first one could be called the case, composed by the longitudinal part, and the second the bulkhead, composed by the top end part.

The propellants (oxidizer and fuel) are mixed and stored within the combustion chamber before flight in solid form, the portion to be burned of propellant is known as grain. Once this mixture is ignited it burns until all propellant is exhausted (Humble *et al.*, 1995) and (Sutton and Biblarz, 2017). The grain surfaces where combustion is undesired are inhibited by a layer of material that protects the grain from the flames, this layer is known as inhibitor. The nozzle is the component responsible for accelerating the combustion gases generated by the grain burn (Huzel and Huang, 1992). This is done by applying the relation between area and velocity for a compressible fluid flowing within a convergent-divergent duct (Anderson, 2003). Furthermore, there is a insulation component, this exist in order to bring a thermal protection to the case and bulkhead, maintaining the structural integrity of the motor. Developing the insulation successfully is of utmost importance to the overall project of a rocket motor (Davenas, 1993) and (I.C.F.S. Vicentin and Araki, 2017).

One of the most simple methods for protecting the motor structure material thermally is the ablative cooling. This method is based in a non-metallic material which have a dual purpose. It provides good heat insulation and when ablated (burned) creates a cool film gas layer next to its surface that protects against the heat of the combustion hot gases (Turner, 2009). This region of the SRM is depicted in Fig. (2).

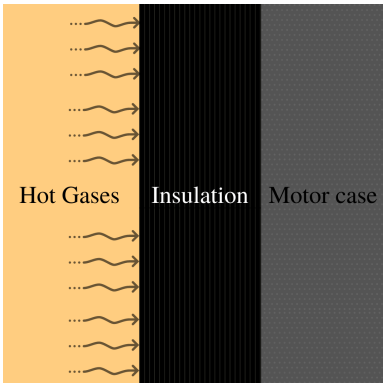

Figure 2. Motor wall close view.

In this work, a open software was developed to solve the transient heat transfer problem applying finite difference method in a discretized domain over the case and bulkhead of the SRM. In addition to that, a Guide User Interface (GUI) with oriented programming was created to provide a rapid and efficient way of analysing the motor temperature aiming the accessibility to rocketry team to obtain multiple data without high level of complexity. Finally, a comparison is made with THERMCAS solver, since this is one of the software commonly used for the same purpose.

2. HEAT TRANSFER PROBLEM

In order to address the SRM heat transfer problem, a cylindrical coordinate system was used. This was chosen to take advantage of the radial symmetry of the rocket motor, coordinate system and model concept can be seen in Fig. (3).

The heat transfer that occurs between a fluid in motion and a bounding surface when the two are at different temperatures is called convection (Incropera *et al.*, 2007). This heat transfer mode happens in the interface between the hot gases and the thermal insulation inside the SRM. The mathematical equation that describes the heat exchanged in this process is known as Newton Law of Cooling, presented in Eq. (1),

$$q_{conv} = h_m(T_\infty - T_w) \tag{1}$$

where h_m stands for convective heat coefficient, that, according to Eugene A. Avallone (1996), for a turbulent flow inside a cylinder is obtained by Eq. (2), where T_∞ is the free-stream temperature and T_w the bounding surface temperature.

$$h_m = 0.024\frac{C_p G^{0.8}}{D_i^{0.2}}\left[1 + \left(\frac{D_i}{L}\right)^{0.7}\right] \tag{2}$$

Where C_p is the specific heat, G the average mass flux, D_i the inner cylinder diameter and L the motor length. The average mass flux is calculated considering that the propellant is burned evenly during the whole specified burn time.

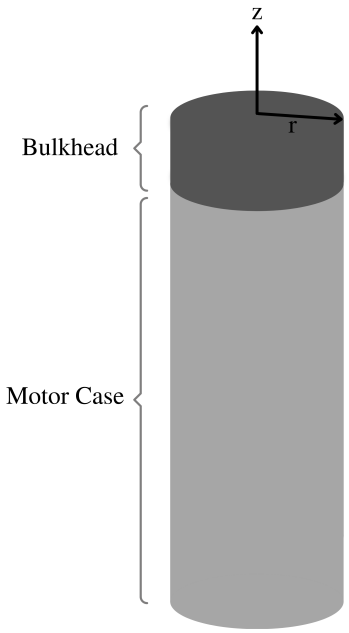

Figure 3. Coordinate system in rocket motor.

Thus, on the insulator and hot gases interface, there is the need to apply the conservation of heat equation, which implies that the change in the total energy inside a fixed volume needs to equal the heat passing through the volume surface. This yields a form of the First Law of Thermodynamics when there is no work being applied to the closed system. In this way, the heat entering is only originate from convection and conduction. On the other way, the change in total energy is equal to the thermal energy (if the material is not passing through a phase change), which is proportional to the product of the density, specific heat and the closed system volume.

$$\rho C_p \frac{\partial T}{\partial t} dV = q_{conv} + q_{cond} \tag{3}$$

Based on experimental evidence, there was derived the Heat Rate Equation (Incropera *et al.*, 2007) where it states that the heat transported trough conduction is proportional to the product of the temperature gradient and the area in contact, Eq. (4).

$$q_{cond} = kdA \frac{\partial T}{\partial r} \tag{4}$$

It is worth noticing that if the conduction is being analyzed in the z coordinate it would be a z instead of a r in Eq. (4), also, k is the thermal conductivity of the material.

The heat transfer within the insulation material and case/bulkhead is done by conduction, that according to (Incropera *et al.*, 2007) is the transfer of energy from the more energetic to the less energetic particles of a substance due to interactions between them. The conduction occurring inside a solid material is related to the temperature variation according to time and space, as shown in Eq. (5).

$$\frac{1}{\alpha}\frac{\partial T}{\partial t} = \frac{\partial^2 T}{\partial r^2} + \frac{1}{r}\frac{\partial T}{\partial r} + \frac{\partial^2 T}{\partial z^2} \tag{5}$$

Equation 5 is often called the Fourier Law in two dimensions, this equation is phenomenological; that is, it is developed from observed phenomena rather than being derived from first principles (Incropera *et al.*, 2007). Where T is the temperature in the solid, t is time, r is the radial coordinate and z is the height of the cylinder coordinate. In order to address the one-dimensional problem it is only necessary to disregard the z coordinate second partial derivative.

2.1 Finite Difference Method

In order to solve the heat transfer problem previously presented a finite difference method (FDM) was implemented. The FDM proceed by replacing the derivatives in the differential equation with a finite difference at evenly spaced mesh points LeVeque (2007). This approach result in a large number of algebraic system of equations that may be easier to solve numerically.

The replacement can be done in several ways, the most common the forward, backward and central approximations based on Taylor series expansion. Therefore, consider the discrete domain x ($x \in [0, L]$) of N points where each i-th point is denoted by x_i as showed in Fig. (4).

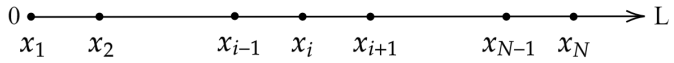

Figure 4. Discrete domain

The objective is to approximate $\frac{dy}{dx}$ in $x = x_i$ and this can be done with Taylor series. The upward approximation of $y(x)$ is

$$y_{i+1} = y_i + (x_{i+1} - x_i)\frac{dy}{dx}\Big|_{x_i} + \frac{(x_{i+1} - xi)^2}{2!}\frac{d^2y}{dx^2}\Big|_{x_i} + \frac{(x_{i+1} - xi)^3}{3!}\frac{d^3y}{dx^3}\Big|_{x_i} + ... \tag{6}$$

If the interval $h = x_{i+1} - x_i$ is close enough, only first order therms are considered Kiusalaas (2005). Manipulating Eq. (6) the general result for upward approximation is obtained in Eq. (7).

$$\frac{dy}{dx}\Big|_{x_i} \approx \frac{y_{i+1} - y_i}{h} \tag{7}$$

Similarly the backward and central scheme can be obtained resulting in Eq. 8 and 9, respectively.

$$\frac{dy}{dx}\Big|_{x_i} \approx \frac{y_i - y_{i-1}}{h} \tag{8}$$

$$\frac{dy}{dx}\Big|_{x_i} \approx \frac{y_{i+1} - y_{i-1}}{2h} \tag{9}$$

The same procedure is reproduced in order to obtain higher derivative order using Eq. 6, (Richard L. Burden, 2010). In this work only first and second (Eq. 10) order will be used.

$$\frac{d^2y}{dx^2}\Big|_{x_i} \approx \frac{y_{i+1} - 2y_i + y_{i-1}}{\Delta x^2} \tag{10}$$

For the heat transfer problem in the rocket motor case, the domain is applied in radial direction and the material properties varies from the radial point, Fig. (5).

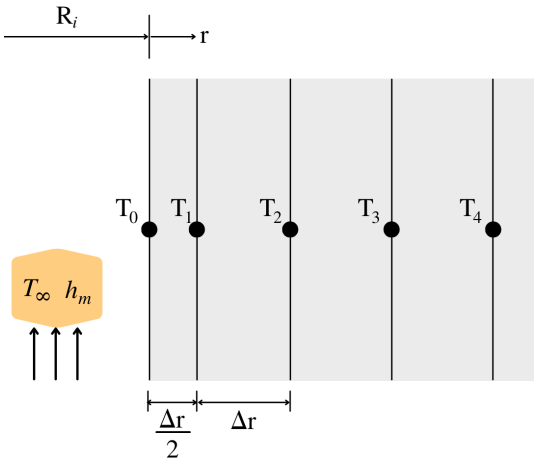

Figure 5. Radial domain in a motor case

Where, R_i stands for the inner radius, the location where the insulation begins in relation to the motor symmetry axis. In bulkhead model it is also taken into consideration the variable z, that would add to every z point a row of radial points. At last, applying FDM to the heat problem results in two possible numerical solutions, implicit and explicit. The implicit solution means a solution where the variable of interest cannot be separable, the opposite occurs in explicit solution.

2.2 Implicit discretization - Case

By applying FDM (Section 2.1) to the heat problem in the case with the right-hand side at the future time, a set of equation is obtained for the Implicit Method solution. It is applied to the first radial coordinate the Conservation of Energy Eq. (3) with upward FDM Eq. (7), to the inner radial coordinate it is used the Fourier Law with central FDM Eq. (9) and to the last radial coordinate also the Fourier Law but with backward FDM Eq. (8).

$$\begin{cases} \rho C_p \frac{\Delta r}{2}\left(\frac{T_j^{i+1}-T_j^i}{\Delta t}\right) = k\left(\frac{T_{j+1}^{i+1}-T_j^{i+1}}{\Delta r}\right) + h_m(T_\infty - T_j^i) & (a) \\ \frac{1}{\alpha}\frac{T_j^{i+1}-T_j^i}{\Delta t} = \frac{T_{j+1}^{i+1}+T_{j-1}^{i+1}-2T_j^{i+1}}{(\Delta r)^2} + \frac{T_{j+1}^{i+1}-T_{j-1}^{i+1}}{2r\Delta r} & (b) \\ \frac{1}{\alpha}\frac{T_j^{i+1}-T_j^i}{\Delta t} = \frac{T_{j-2}^{i+1}+T_j^{i+1}-2T_{j-1}^{i+1}}{(\Delta r)^2} + \frac{T_j^{i+1}-T_{j-1}^{i+1}}{r\Delta r} & (c) \end{cases} \tag{11}$$

Therefore, opening and regrouping the terms presented in Eq. (11) results in three equations for first, inner and last radial coordinate in Eq. (12).a, (12).b and (12).c, respectively.

$$\begin{cases} \left(1-\frac{h_m 2\Delta t}{\rho\Delta C_p}\right)T_j^i + \frac{h_m 2\Delta t T_\infty}{\Delta r \rho c_p} = \left(1+\frac{2k\Delta t}{\rho C_p \Delta r^2}\right)T_j^{i+1} + \left(\frac{-2k\Delta t}{\rho C_p \Delta r^2}\right)T_{j+1}^{i+1} & (a) \\ T_j^i = \left(1+\frac{2\alpha\Delta t}{(\Delta r)^2}\right)T_j^{i+1} + \left(\frac{\alpha\Delta t}{2r\Delta r} - \frac{\alpha\Delta t}{(\Delta r)^2}\right)T_{j-1}^{i+1} - \left(\frac{\alpha\Delta t}{2r\Delta r} + \frac{\alpha\Delta t}{(\Delta r)^2}\right)T_{j+1}^{i+1} & (b) \\ T_j^i = \left(1-\frac{\alpha\Delta t}{(\Delta r)^2} - \frac{\alpha\Delta t}{r\Delta r}\right)T_j^{i+1} + \left(\frac{2\alpha\Delta t}{(\Delta r)^2+\frac{\alpha\Delta t}{r\Delta r}}\right)T_{j-1}^{i+1} - \left(\frac{\alpha\Delta t}{(\Delta r)^2}\right)T_{j-2}^{i+1} & (c) \end{cases} \tag{12}$$

As can be seen in Eq. (12), the Implicit Finite Difference Method created a system of algebraic equations that gave the previous temperature at the node based on the future temperature of the node and its surroundings (Incropera *et al.*, 2007). In order to solve this system the inverse matrix of the coefficients multiplying the new temperatures was calculated and then multiplied with the known temperatures vector to achieve the new temperature vector.

In Eq. (11) and (12) α is the thermal diffusivity, Δr is the radial step, Δt is the time step and T is the temperature in the $i-th$ time step and $j-th$ radial step.

2.3 Explicit discretization - Case

In the other hand, applying FDM to the problem it is also possible to obtain a set of equations in order to solve by explicit method. Also, the domain is shown in Fig. (5) and in a similar way to the implicit discretization there are three equations, one for first, inner and last radial coordinate Eq. (14).

$$\begin{cases} \rho C_p \frac{\Delta r}{2}\left(\frac{T_j^{i+1}-T_j^i}{\Delta t}\right) = k\left(\frac{T_{j+1}^{i}-T_j^{i}}{\Delta r}\right) + h_m(T_\infty - T_j^i) & (a) \\ \frac{1}{\alpha}\frac{T_j^{i+1}-T_j^i}{\Delta t} = \frac{T_{j+1}^{i}+T_{j-1}^{i}-2T_j^{i}}{(\Delta r)^2} + \frac{T_{j+1}^{i}-T_{j-1}^{i}}{2r\Delta r} & (b) \\ \frac{1}{\alpha}\frac{T_j^{i+1}-T_j^i}{\Delta t} = \frac{T_{j}^{i}+T_{j-2}^{i}-2T_{j-1}^{i}}{(\Delta r)^2} + \frac{T_{j}^{i}-T_{j-1}^{i}}{r\Delta r} & (c) \end{cases} \tag{13}$$

$$\begin{cases} T_j^{i+1} = \left(1-\frac{2k\Delta t}{\rho C_p \Delta r^2} - \frac{2h_m\Delta t}{\rho C_p \Delta r}\right)T_j^i + \left(\frac{2k\Delta t}{\rho C_p \Delta r^2}\right)T_{j+1}^i + \frac{2h_m T_\infty \Delta t}{\rho C_p \Delta r} & (a) \\ T_j^{i+1} = \left(1-\frac{2\alpha\Delta t}{(\Delta r)^2}\right)T_j^i + \left(\frac{\alpha\Delta t}{(\Delta r)^2} - \frac{\alpha\Delta t}{2r\Delta r}\right)T_{j-1}^i + \left(\frac{\alpha\Delta t}{2r\Delta r} + \frac{\alpha\Delta t}{(\Delta r)^2}\right)T_{j+1}^i & (b) \\ T_j^{i+1} = \left(1+\frac{\alpha\Delta t}{(\Delta r)^2} + \frac{\alpha\Delta t}{r\Delta r}\right)T_j^i - \left(\frac{\alpha\Delta t}{r\Delta r} + \frac{2\alpha\Delta t}{(\Delta r)^2}\right)T_{j-1}^i + \left(\frac{\alpha\Delta t}{(\Delta r)^2}\right)T_{j-2}^i & (c) \end{cases} \tag{14}$$

In the Explicit Finite Difference Method the future temperature of a node is only dependent on previously known temperatures in its surroundings Incropera *et al.* (2007), so it is possible to solve the temperature for each node at a given time. This process can be computationally costly since it needs a finer mesh to converge due to stability criteria.

Otherwise, implicit method can also be computationally costly due to matrix size to be inverted and the inversion method also can be fundamental to determine the solver time cost. Considering this work, there will be a small number of nodes, turning the implicit approach faster than the explicit one.

In Eq. (13) and (14) T is the temperature in the $i-th$ time step and $j-th$ radial step.

2.4 Explicit discretization - Bulkhead

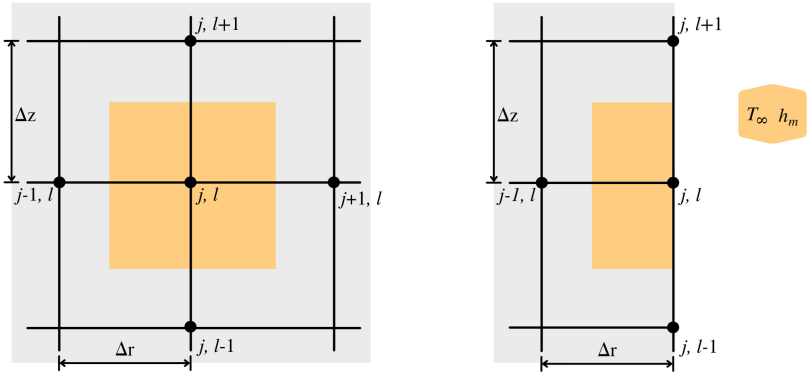

Figure 6. Cylindrical domain in motor bulkhead

The bulkhead model makes use of the same set of equations used to develop the case discretized equations, the only difference is that now the z coordinate is taken into consideration. It produces six more equations for the entire domain Fig. (6), that are presented in Eq. (15 to 23). For the bulkhead, only the explicit method is easily implemented, the reason for this is that to solve the equation implicitly it is required to solve simultaneously for nodes varying in r and z, which could not be done by the ease it was done in the one-dimension scheme. Eq. (15 to 17) represent the temperature equations to the first z point for respectively, first, inner and last r points.

$$\frac{\rho C_p \Delta r \Delta z}{4}\left(\frac{T_{j,l}^{i+1}-T_{j,l}^{i}}{\Delta t}\right)=\frac{k\Delta z}{2}\left(\frac{T_{j+1,l}^{i}-T_{j,l}^{i}}{\Delta r}\right)+\frac{k\Delta r}{2}\left(\frac{T_{j,l+1}^{i}-T_{j,l}^{i}}{\Delta z}\right)+\frac{h_m\Delta r}{2}(T_\infty-T_{j,l}^{i}) \tag{15}$$

$$\frac{\rho C_p \Delta r \Delta z}{2}\left(\frac{T_{j,l}^{i+1}-T_{j,l}^{i}}{\Delta t}\right)=\frac{k\Delta z}{2}\left(\frac{T_{j+1,l}^{i}-T_{j-1,l}^{i}}{\Delta r}\right))+k\Delta r\left(\frac{T_{j,l+1}^{i}-T_{j,l}^{i}}{\Delta z}\right)+h_m\Delta r(T_\infty-T_{j,l}^{i}) \tag{16}$$

$$\frac{\rho C_p \Delta r \Delta z}{4}\left(\frac{T_{j,l}^{i+1}-T_{j,l}^{i}}{\Delta t}\right)=\frac{k\Delta z}{2}\left(\frac{T_{j,l}^{i}-T_{j-1,l}^{i}}{\Delta r}\right)+\frac{k\Delta r}{2}\left(\frac{T_{j,l+1}^{i}-T_{j,l}^{i}}{\Delta z}\right)+\frac{h_m\Delta r}{2}(T_\infty-T_{j,l}^{i}) \tag{17}$$

Equations (18 to 20) represent the temperature equations to the inner z point for respectively, first, inner and last r points.

$$\frac{1}{\alpha}\frac{T_{j,l}^{i+1}-T_{j,l}^{i}}{\Delta t}=\frac{T_{j+2,l}^{i}+T_{j,l}^{i}-2T_{j+1,l}^{i}}{(\Delta r)^2}+\frac{T_{j+1,l}^{i}-T_{j,l}^{i}}{r\Delta r}+\frac{T_{j,l+1}^{i}+T_{j,l-1}^{i}-2T_{j,l}^{i}}{(\Delta z)^2} \tag{18}$$

$$\frac{1}{\alpha}\frac{T_{j,l}^{i+1}-T_{j,l}^{i}}{\Delta t}=\frac{T_{j+1,l}^{i}+T_{j-1,l}^{i}-2T_{j,l}^{i}}{(\Delta r)^2}+\frac{T_{j+1,l}^{i}-T_{j-1,l}^{i}}{2r\Delta r}+\frac{T_{j,l+1}^{i}+T_{j,l-1}^{i}-2T_{j,l}^{i}}{(\Delta z)^2} \tag{19}$$

$$\frac{1}{\alpha}\frac{T_{j,l}^{i+1}-T_{j,l}^{i}}{\Delta t}=\frac{T_{j-2,l}^{i}+T_{j,l}^{i}-2T_{j-1,l}^{i}}{(\Delta r)^2}+\frac{T_{j,l}^{i}-T_{j-1,l}^{i}}{r\Delta r}+\frac{T_{j,l+1}^{i}+T_{j,l-1}^{i}-2T_{j,l}^{i}}{(\Delta z)^2} \tag{20}$$

Equations 21 to 23 represent the temperature equations to the last z point for respectively, first, inner and last r points.

$$\frac{1}{\alpha}\frac{T_{j,l}^{i+1}-T_{j,l}^{i}}{\Delta t}=\frac{T_{j+2,l}^{i}+T_{j,l}^{i}-2T_{j+1,l}^{i}}{(\Delta r)^2}+\frac{T_{j+1,l}^{i}-T_{j,l}^{i}}{r\Delta r}+\frac{T_{j,l}^{i}+T_{j,l-2}^{i}-2T_{j,l-1}^{i}}{(\Delta z)^2} \tag{21}$$

$$\frac{1}{\alpha}\frac{T_{j,l}^{i+1}-T_{j,l}^{i}}{\Delta t}=\frac{T_{j+1,l}^{i}+T_{j-1,l}^{i}-2T_{j,l}^{i}}{(\Delta r)^2}+\frac{T_{j+1,l}^{i}-T_{j-1,l}^{i}}{2r\Delta r}+\frac{T_{j,l}^{i}+T_{j,l-2}^{i}-2T_{j,l-1}^{i}}{(\Delta z)^2} \tag{22}$$

$$\frac{1}{\alpha}\frac{T_{j,l}^{i+1}-T_{j,l}^{i}}{\Delta t}=\frac{T_{j-2,l}^{i}+T_{j,l}^{i}-2T_{j-1,l}^{i}}{(\Delta r)^2}+\frac{T_{j,l}^{i}-T_{j-1,l}^{i}}{r\Delta r}+\frac{T_{j,l}^{i}+T_{j,l-2}^{i}-2T_{j,l-1}^{i}}{(\Delta z)^2} \tag{23}$$

2.5 Explicit Method Stability

Solving a Partial Differential Equation (PDE) by the Finite Difference Method and utilizing an Explicit approach requires a stability criterion to be respected for the solution to converge. This criterion, for a parabollic PDE, is, according to the Von Neumann necessary condition for stability, that the coefficient of the associated node of interest at the previous time is greater than or equal to zero (K. W. Morton, 2005).

For the one-dimensional solution, applied to the motor case model, this condition gives the following relation between the finite step in time and the finite step in space.

$$\Delta t \leq \frac{(\Delta r)^2}{2\alpha} \tag{24}$$

The same criteria can be analyzed for the two-dimensional solution of the bulkhead model, and after comparing the results for all the coefficients among Eq. (15 to 23) the smallest is for Eq. (19). In that case, the expression is

$$\Delta t \leq \frac{(\Delta z \Delta r)^2}{2\alpha(\Delta r^2+\Delta z^2)} \tag{25}$$

3. SOFTWARE ARCHITECTURE

The software was developed using Python language due it facilities in scientific computation and the oriented programming paradigm embed into it, turning the software architecture dynamically favorable. The architecture of RTA software is based on four different classes, one responsible for the GUI, one for custom material creation (optional feature) and two other for case and bulkhead solution, as shown in Fig. (7).

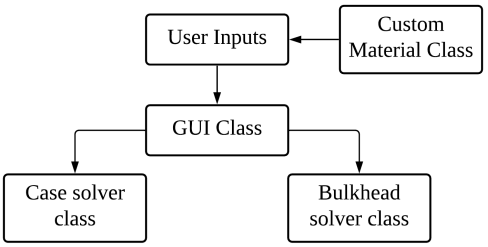

Figure 7. Main classes with user inputs of RTA

For each class there is a series of methods and for simplicity the software architecture is shown in Fig. (8) as an simpler Unified Modeling Language (UML). Custom case and insulation material methods are responsible for the creation of user custom insulation and case materials, setting data such as density, thermal conductivity and specific heat. Display messages methods are responsible for warn user during the simulation. Run h_m function is responsible to calculate the convective heat coefficient according to Eq. (2). Also, it is possible to generate a PDF report with all the calculations done in this method. Run case solver calculates all the simulation in case section in two different methods, explicit and implicit, as detailed in section 2. Run bulkhead solver calculates the simulation in bulkhead motor section using a explicit method. Generate graphs methods display the result in a graphical form depending on the simulation. For case section it is generated three different graphs, one with the temperature distribution in the case radial section at burnout, other containing insulation and case section at burnout and the last contain the case thermal distribution in 25%, 50%, 75% and 100% of burning time. For bulkhead only one graph is explored with vertical thermal distribution. Generate outputs save the results of the simulation with the entire entries and solution.

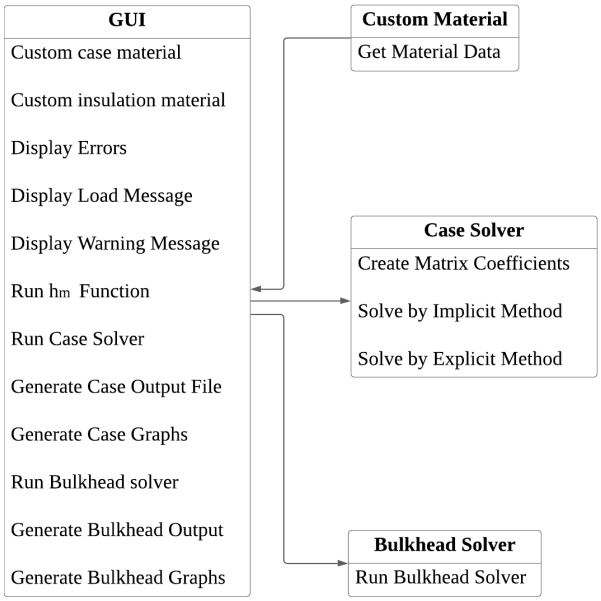

Figure 8. UML for RTA

4. RESULTS

Implementing the software based on sections 2. and 3. results in a quantity of material to be analysed. Since this is a theoretical work, comparisons with THERMCAS was made, a software widely used for thermal analysis in rocket motors. Moreover, stability analysis were made in order to verify the convergence of RTA explicit solution.

4.1 STABILITY ANALYSIS

According to equations 24 and 25, there is a criterion in order to maintain the stability and converge the solution of the parabolic PDE. In order to verify this, it was generated continuous simulation with different time and radial step, and analysing the case wall of rocket motor, the result can be verified in Fig. (9) For 200 time steps the solution already has a

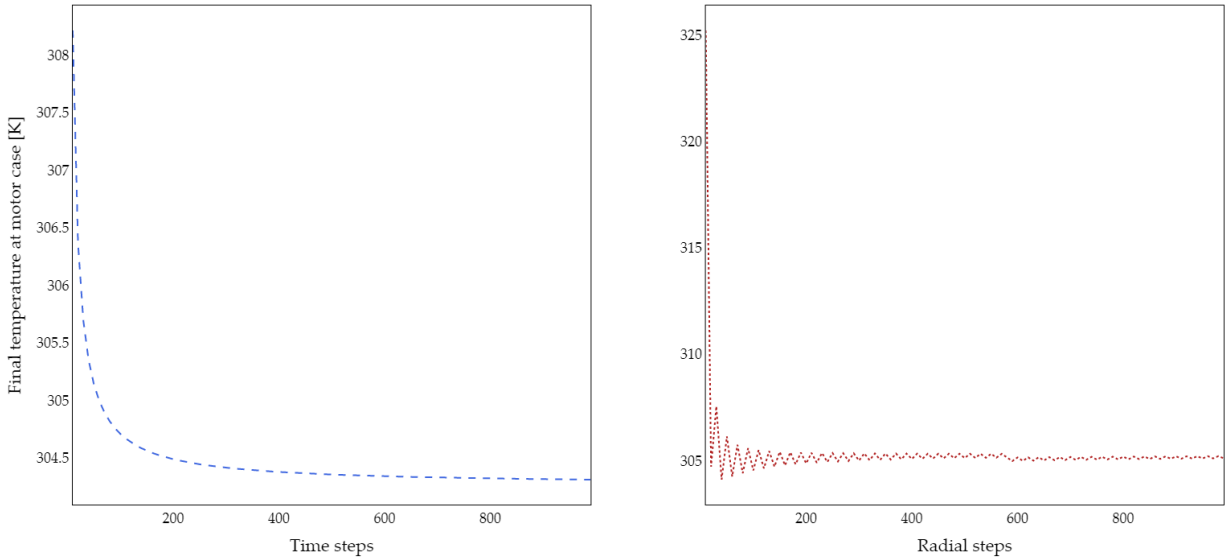

Figure 9. Convergence of the solution varying time and space steps.

good precision, being it deviated by 0.1 from the limit result at that point. For the amplitude of the radial steps temperature oscillation to remain approximately constant it is required about 300 steps, the result will be approximately 0.5 Kelvin deviated from the limit result.

4.2 COMPARISONS

A case study was simulated in order to compare the temperature distribution along the radial coordinate of the motor case with an already used software known as THERMCAS, where also the transient thermal problem is solved. In Fig. (10) it is possible to analyse the implicit and explicit result provided by RTA, in addition to that, there is the result provided by THERMCAS.

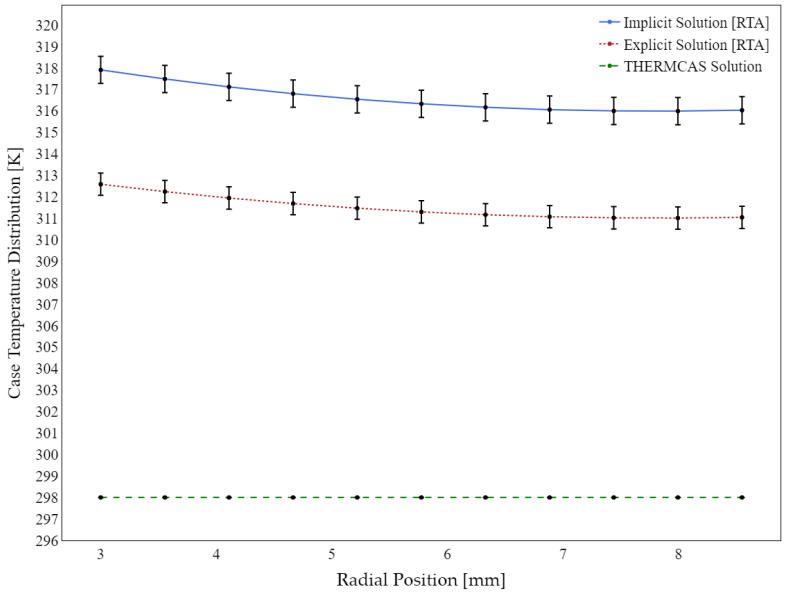

Figure 10. Comparison result of RTA and THERMCAS for a study case.

In THERMCAS, the outputs are rounded, so for the first point of the casing to the last temperature did not change one degree Celsius. This seems unreasonable for the inputs provided. These clearly different results came from the fact that the two approaches to the problem are different. Since THERMCAS considers the coordinate system as cartesian, an evidence is that the software does not ask for the radius of the combustion chamber, so the model is an infinite plane. Also, THERMCAS utilizes the Bender-Schmidt method for solving the transient heat equation, this can imply considerable simplification of the numerical solution (A. N. Mohamad, 2017) therms and probably the main source of difference between the two results. In the other way, at RTA the coordinate system is cylindrical, so the model is an infinite cylinder where is has a greater agreement with rocket motor problem and it consider a more complex solver.

5. Conclusion

Based on the theory and results showed in the previous section, the main purpose of this work was achieved as expected, even showing a greater performance compared to other thermal software available online. The final GUI can be seen in Fig. (11) which it is available for download as an open source software to help other rocketry teams.

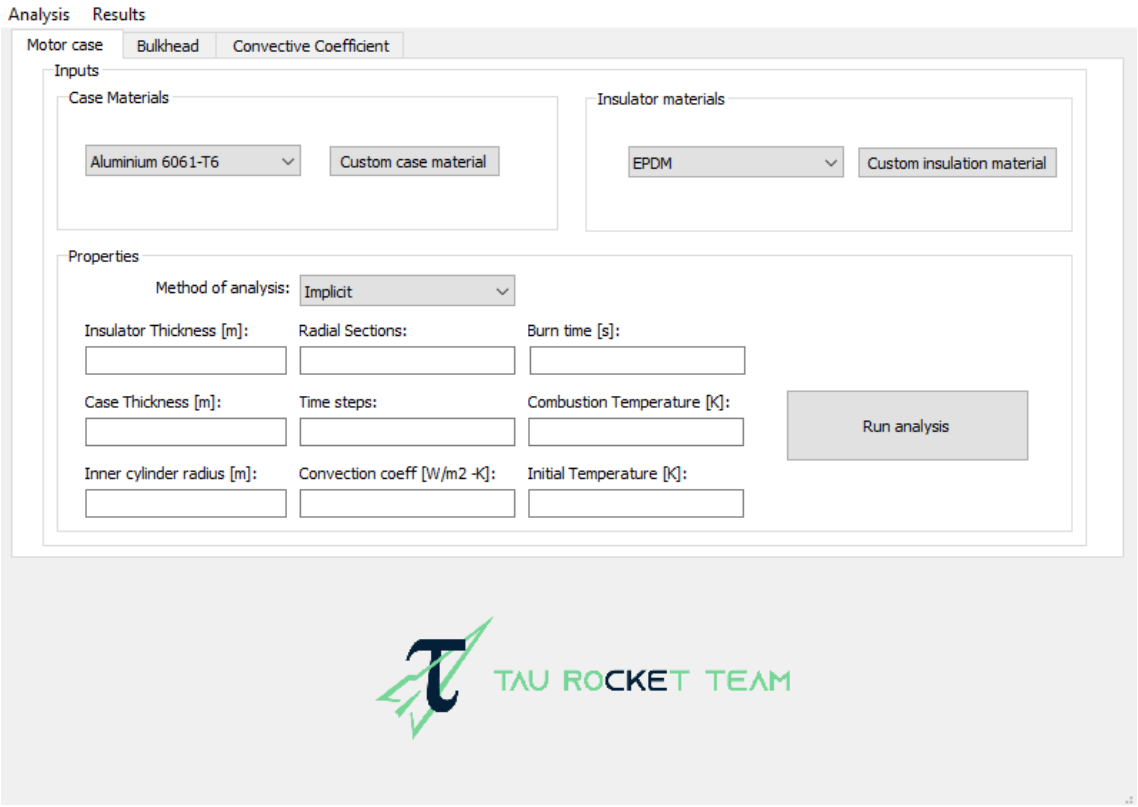

Figure 11. Final GUI of RTA.

6. REFERENCES

A. N. Mohamad, S.F., 2017. *Effect and Efficient Approach of Solving Heat Equation by Different Numerical Approaches Including Crank-Nicolson Schmidt (Method) Which is Still Acting as a Major Role*. International Journal of Advanced Research in Engineering and Applied Sciences.

Anderson, J.D., 2003. *Modern Compressible Flow With Historical Perspective*. Mc Graw Hill, New York, New York.

Davenas, A., 1993. *Solid Rocket Propulsion Technology*. Pergamon Press, Oxford, England.

Eugene A. Avallone, T.B.I., 1996. *Mark's Standard Handbook for Mechanical Engineers*. McGraw-Hill, 10^{th} edition.

Humble, R.W., Henry, G.N. and Larson, W.J., 1995. *Space Propulsion Analysis and Design*. McGraw-Hill, United States of America.

Huzel, D.K. and Huang, D.H., 1992. *Modern Engineering for Design of Liquid-propellant Rocket Engines*. American Institute of Aeronautics and Astronautics, Washington, DC.

I.C.F.S. Vicentin, C.H. Marchi, A.F.D.M.N.S.M.C. and Araki, L., 2017. "Theoretical and experimental heat transfer in rocket engine with solid propellant". *COBEM*.

Incropera, F.P., Dewitt, D.P., Bergman, T.L. and Lavine, A.S., 2007. *Fundamentals of Heat and Mass Transfer*. John Wiley & Sons, Hoboken, New Jersey, 6^{th} edition.

K. W. Morton, D.M., 2005. *Numerical Solution of Partial Differential Equations*. Cambridge University Press, 2^{nd} edition.

Kiusalaas, J., 2005. *Numerical Methods in Engineering with Python*. Cambridge University Press, New York, EUA.

LeVeque, R.J., 2007. *Finite Difference Methods for Ordinary and Partial Differential Equations*. Society for Industrial and Applied Mathematics, Philadelphia, EUA.

Richard L. Burden, J.D.F., 2010. *Numerical Analysis*. Brooks/Cole, Cengage Learning, 9^{th} edition.

Sutton, G.P. and Biblarz, O., 2017. *Rocket Propulsion Elements*. Wiley, Hoboken, New Jersey, 9^{th} edition.

Turner, M.J.L., 2009. *Rocket and Spacecraft Propulsion*. Springer, Praxis, Chichester, United Kingdom.

White, F., 2018. *The overview Effect: Space Exploration and Human Evolution*. American Institute of Aeronautics and Astronautics, 3^{rd} edition.

7. RESPONSIBILITY NOTICE

The following text, properly adapted to the number of authors, must be included in the last section of the paper: The author(s) is (are) solely responsible for the printed material included in this paper.